Systematic study of breakup effects on complete fusion at energies above the Coulomb barrier

Bing Wang,[1] Wei-Juan Zhao,[1] P. R. S. Gomes,[2] En-Guang Zhao,[3, 4] and Shan-Gui Zhou[3, 4, 5, *]

[1]*Department of Physics, Zhengzhou University, Zhengzhou 450001, China*
[2]*Instituto de Física, Universidade Federal Fluminense,*
Avenida Litoranea s/n, Gragoatá, Niterói, Rio de Janeiro, 24210-340, Brazil
[3]*State Key Laboratory of Theoretical Physics, Institute of Theoretical Physics,*
Chinese Academy of Sciences, Beijing 100190, China
[4]*Center of Theoretical Nuclear Physics, National Laboratory of Heavy Ion Accelerator, Lanzhou 730000, China*
[5]*Center for Nuclear Matter Science, Central China Normal University, Wuhan 430079, China*
(Dated: July 30, 2017)

A large number of complete fusion excitation functions of reactions including the breakup channel were measured in recent decades, especially in the last few years. It allows us to investigate the systematic behavior of the breakup effects on the complete fusion cross sections. To this end, we perform a systematic study of the breakup effects on the complete fusion cross sections at energies above the Coulomb barrier. The reduced fusion functions $F(x)$ are compared with the universal fusion functions which are used as a uniform standard reference. The complete fusion cross sections at energies above the Coulomb barrier are suppressed by the breakup of projectiles. This suppression effect for reactions induced by the same projectile is independent of the target and mainly determined by the lowest energy breakup channel of the projectile. There holds a good exponential relation between the suppression factor and the energy corresponding to the lowest breakup threshold.

PACS numbers: 25.60.Pj, 24.10.-i, 25.70.Mn, 25.70.Jj

I. INTRODUCTION

In recent years, the investigation of breakup effects on fusion reactions in heavy-ion collisions around the Coulomb barrier has been a subject of intense experimental and theoretical interests [1–3]. Various processes can take place after the projectile breaks up. One is the incomplete fusion (ICF) in which part of the fragments is absorbed by the target. When all the fragments fuse with the target, the process is called sequential complete fusion (SCF). From the experimental point of view, the SCF cannot be distinguished from the direct complete fusion (DCF) in which the whole projectile fuses with the target without breakup. Therefore, only the complete fusion (CF) cross section, which includes both DCF and SCF cross sections, can be measured.

The total fusion (TF) cross section is the sum of the CF and ICF cross sections, $\sigma_{\mathrm{TF}} \equiv \sigma_{\mathrm{CF}} + \sigma_{\mathrm{ICF}}$. Experimentally, it is difficult to measure separately ICF and CF cross sections. Especially for light reaction systems, the excited compound nucleus emits charged particles during the cooling process. The residues from ICF cannot be distinguished from those from CF, and hence only the TF cross section can be measured. The situation is different in the case of heavy reaction systems, because the decay of the excited compound nucleus through the emission of charged particles can be negligible and the separate measurements of the CF cross section can be achieved. Many measurements of the CF cross sections have been performed [4–14].

Several methods have been adopted to investigate the influence of the breakup on fusion reactions around the Coulomb barrier [15–20]. One of the most widely employed approaches is to compare the data with either the predictions of coupled channel (CC) calculations without the breakup channels [10, 11, 21–25] or the predictions of a single barrier penetration model (SBPM) [5, 12–14]. It was found that the CF cross sections are suppressed at energies above the Coulomb barrier. In Refs. [13, 26], it was concluded that the CF suppression for the reactions involving ^{6}Li, ^{7}Li, and ^{10}B projectiles is almost independent of the target charge by comparing the CF data with the predictions of CC or SBPM calculations, and the suppression shows a remarkably consistent correlation with the breakup threshold energy. Sargsyan *et al.* [19] investigated the systematic behavior for the CF suppression as a function of the target charge and bombarding energy by using the quantum diffusion approach. In Ref. [17], the influence of breakup effects on CF cross sections for ^{9}Be induced reactions were discussed by applying the universal fusion function formalism and it was concluded that there is not a clear systematic behavior of the CF suppression as a function of the target charge.

As mentioned above, the conclusions concerning the CF suppression obtained by different methods are different. Therefore, further systematic study of the influence of the breakup on CF cross sections is needed. Particularly, in the last few years, new experiments with weakly bound nuclei were performed and the corresponding CF cross sections were measured [21–25]. Moreover, evidences of breakup for tightly bound projectiles (^{11}B, ^{12,13}C and ^{16}O) were also found [14, 27–30]. It allows us to explore the breakup effects on CF cross sections in a

wider range.

In order to perform a systematic study of the breakup effects on CF cross sections, it is necessary to reduce the data to eliminate the geometrical factors in different reaction systems [31]. After the reduction, the data should be compared with the theoretical predictions without taking into account the coupling of the breakup channel.

Several reduction methods have been used to reduce the data [32–37]. In this paper, the one proposed in Refs. [35, 36], which can eliminate completely the geometrical factors and static effects of the potential between the two nuclei, is employed to reduce the CF data. We will explore the influence of the breakup on CF cross sections at energies above the Coulomb barrier, because the coupling channel effects except the breakup do not play a significant role on fusion cross sections in this energy range [38, 39]. Meanwhile, in order to avoid using a very large diffuseness parameter in the Woods-Saxon potential [40, 41], we choose the double folding and parameter-free São Paulo potential (SPP) [42–44] as the interaction potential between the projectile and the target. The SPP has been widely and successfully used in the study of heavy-ion reactions [45–50]. The universal fusion function (UFF) [35, 36] will be used as a uniform standard reference with which the reduced data can be compared directly.

The present paper is organized as follows. In Sec. II the method used to eliminate geometrical factors and static effects of the data and the SPP are introduced. This method is applied to analyze the data of different projectiles induced reactions in Sec. III where the systematics of the suppression effects from the breakup channel will be investigated. A summary is given in Sec. IV.

II. METHODS

In order to study the systematic behavior of the breakup effects on CF cross sections, it is necessary to eliminate completely the geometrical factors and static effects of the potential between the two nuclei. We adopt the method proposed in Refs. [35, 36]. According to this prescription, the fusion cross section and the collision energy are reduced to a dimensionless fusion function $F(x)$ and a dimensionless variable x,

$$F(x) = \frac{2E_{\text{c.m.}}}{R_{\text{B}}^2 \hbar \omega} \sigma_{\text{F}}, \quad x = \frac{E_{\text{c.m.}} - V_{\text{B}}}{\hbar \omega}, \quad (1)$$

where $E_{\text{c.m.}}$ is the collision energy in the center of mass frame, σ_{F} is the fusion cross section, and R_{B}, V_{B}, and $\hbar \omega$ denote the radius, height, and curvature of the barrier which is approximated by a parabola. The barrier parameters R_{B}, V_{B}, and $\hbar \omega$ are obtained from the SPP.

In the model of SPP, the nuclear interaction V_{N} is given as [42–44]

$$V_{\text{N}}(R, E_{\text{c.m.}}) \approx V_{\text{F}}(R) \exp\left(-\frac{4v^2}{c^2}\right), \quad (2)$$

where V_{F} is the double-folding potential obtained by using the density distributions of the nuclei. The two-parameter Fermi distribution is used to describe the densities of the nuclei. c denotes the speed of light, and v the relative velocity between the projectile and the target,

$$v(R, E_{\text{c.m.}}) = \sqrt{2[E_{\text{c.m.}} - V_{\text{C}}(R) - V_{\text{N}}(R, E_{\text{c.m.}})]/\mu}. \quad (3)$$

V_{C} is the Coulomb potential which is also calculated through a folding procedure. μ is the reduced mass of the reaction system in question.

The reduction method given by Eq. (1) is inspired by the Wong's formula [51],

$$\sigma_{\text{F}}^{\text{W}}(E_{\text{c.m.}}) = \frac{R_{\text{B}}^2 \hbar \omega}{2E_{\text{c.m.}}} \ln \left[1 + \exp\left(\frac{2\pi(E_{\text{c.m.}} - V_{\text{B}})}{\hbar \omega}\right) \right]. \quad (4)$$

If the fusion cross section can be accurately described by the Wong's formula, the $F(x)$ reduces to

$$F_0(x) = \ln\left[1 + \exp(2\pi x)\right], \quad (5)$$

which is called the UFF [35, 36]. Note that $F_0(x)$ is a general function of the dimensionless variable x and independent of reaction systems. It is well known that the Wong's formula has limitations and does not describe properly the behavior of fusion cross sections of light systems at sub-barrier energies. However, in the present work we are dealing with energies above the barrier, an energy region where the Wong's formula can be applied. In particular, when $x > 1$, one has $F_0(x) \approx 2\pi x$. Then the fusion cross section is calculated as

$$\sigma_{\text{F}} = \pi R_{\text{B}}^2 (E_{\text{c.m.}} - V_{\text{B}})/E_{\text{c.m.}}. \quad (6)$$

Thus, fusion becomes independent on the width of the barrier and can be described as the absorption by a black disc of radius R_{B}. Partial fusion, producing the reduction of the complete fusion, can be visualized as coming from one of the breakup fragments not falling into the black disc. So, the $F_0(x)$ is used as a uniform standard reference to explore the breakup effects on CF cross sections.

Using the above reduction procedure, the CF data for different reaction systems can be compared directly and the systematics can be investigated. Deviations of the fusion function, if exist, from the UFF at energies above the Coulomb barrier mainly arise from the effects of the breakup on CF cross sections [38, 39], because inelastic excitations and transfer channel couplings are not important at energies above the Coulomb barrier. This is also the reason why one does not need to renormalize the experimental fusion functions, as prescribed by Canto *et al.* [35, 36].

III. RESULTS AND DISCUSSIONS

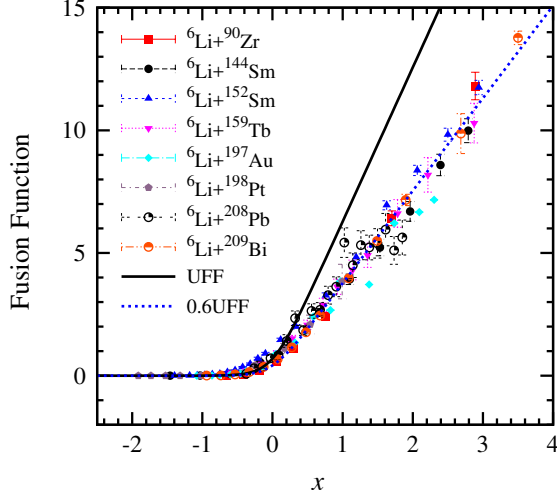In the last few years, CF cross sections for many reactions involving weakly bound nuclei have been measured

FIG. 1. (Color online) The complete fusion function $F(x)$ for the weakly bound projectile ^{6}Li on different target nuclei as a function of x. The solid line represents the UFF [Eq. (5)] and the dotted line is the UFF multiplied by the suppression factor $F_{\text{B.U.}} = 0.60$ [cf. Eq. (7)]. The experimental values are taken from Refs. [21] (^{90}Zr), [11] (^{144}Sm), [22] (^{152}Sm), [23] (^{159}Tb), [24] (^{197}Au), [8] (^{198}Pt), [6] (^{208}Pb), and [10] (^{209}Bi).

[21–25]. The suppression of complete fusion cross sections above the Coulomb barrier due to the breakup has been observed in these reaction systems. More interestingly, for tightly bound projectiles (^{11}B, ^{12,13}C and ^{16}O), the evidence for incomplete fusion has been also found [14, 27–30]. This fact allows us to explore the influence of the breakup on CF cross sections in a wider range of projectiles and breakup threshold energies. We collected the CF data for reactions induced by ^{6,7}Li, ^{9}Be, ^{10,11}B, ^{12,13}C, and ^{16}O which are shown in Table I. Based on the reduction method mentioned above, we first investigate the influence of breakup effects on the CF cross sections for each projectile. Then we study the systematic behavior of the suppression factors for different projectiles.

A. Complete fusion functions for reactions involving weakly and tightly bound projectiles

The CF functions for the weakly bound projectile ^{6}Li on different target nuclei as a function of x are illustrated in Fig. 1. The most favorable breakup channel for ^{6}Li is ^{6}Li $\rightarrow \alpha + d$ owing to the lowest separation energy of 1.474 MeV. The solid line represents the UFF, i.e., $F_0(x)$ given in Eq. (5). On the one hand, it can be seen from Fig. 1 that all of CF functions are below the UFF at energies above the Coulomb barrier and one can conclude that the CF cross sections are suppressed at energies above the Coulomb barrier compared with the UFF. On the other hand, it seems that the suppression is almost independent of the target, at least for masses larger than 90. We introduce a suppression factor $F_{\text{B.U.}}$

TABLE I. The reactions studied in this work. The first and last column denote the projectile (Proj.) and target (Targ.) of the reaction, respectively. The second column represents the lowest breakup threshold $E_{\text{B.U.}}$ (in MeV) for the projectile. The suppression factors $F_{\text{B.U.}}$ obtained by fitting the CF functions are listed in the third column. The $F_{\text{B.U.}}^{\text{em}}$ denotes the suppression factor obtained from the empirical formula (9). The suppression factors taken from the literature are given in the fifth column and the corresponding references are shown in the last column.

Proj.	$E_{\text{B.U.}}$ (MeV)	$F_{\text{B.U.}}$ (fit)	$F_{\text{B.U.}}^{\text{em}}$ [Eq. (9)]	$F_{\text{B.U.}}$ (Refs.)	Targ.
^{6}Li	1.474	0.60	0.601	0.66 ± 0.08	^{90}Zr [21]
				0.68	^{144}Sm [11]
				0.72 ± 0.04	^{152}Sm [22]
				0.66 ± 0.05	^{159}Tb [23]
				0.65 ± 0.23	^{197}Au [24]
					^{198}Pt [8]
					^{208}Pb [6]
				$0.66^{+0.05}_{-0.04}$	^{209}Bi [10]
^{7}Li	2.467	0.67	0.690	0.75 ± 0.04	^{144}Sm [25]
				0.75 ± 0.04	^{152}Sm [25]
				0.74	^{159}Tb [4]
				0.70	^{165}Ho [5, 12]
				0.85 ± 0.04	^{197}Au [24]
					^{198}Pt [52]
				$0.74^{+0.03}_{-0.02}$	^{209}Bi [10]
^{9}Be	1.573	0.68	0.612	0.80 ± 0.04	^{89}Y [28]
				0.90	^{144}Sm [7, 53]
				0.72	^{124}Sn [54]
				0.60	^{186}W [9]
				$0.70^{+0.08}_{-0.07}$	^{208}Pb [10]
				0.68	^{209}Bi [55, 56]
^{10}B	4.461	0.80	0.799	0.86	^{159}Tb [57]
				0.85	^{209}Bi [13]
^{11}B	8.665	0.91	0.916		^{159}Tb [57]
				0.93	^{209}Bi [13]
^{12}C	7.367	0.88	0.890		^{89}Y [28]
					^{152}Sm [4]
					^{159}Tb [30]
					^{181}Ta [58]
				0.88	^{208}Pb [14]
^{13}C	10.648	0.94	0.943		^{159}Tb [29]
					^{181}Ta [58]
				0.97	^{207}Pb [14]
^{16}O	7.162	0.87	0.885		^{103}Rh [59]
					^{148}Nd [4]
					^{150}Nd [4]
					^{159}Tb [27]
					^{169}Tm [27]

as,

$$F_{\text{B.U.}} = \frac{F(x)}{F_0(x)}. \qquad (7)$$

$F_{\text{B.U.}}$ is obtained by fitting the experimental fusion functions $F(x)$ with $x > 0$. In Fig. 1, the dotted line represents the UFF multiplied by the $F_{\text{B.U.}}$ of 0.6. The $F_{\text{B.U.}}$

of 0.6 is consistent with the results taken from the literature which are listed in the fifth column of Table I. These results were obtained by comparing the CF data with the coupled channel calculations. One can find that all the CF functions are very close to the dotted line, which implies that the suppression factors for the ^{6}Li projectile with different targets are almost the same. Consequently, the suppression factors for ^{6}Li induced reactions are independent of the charge of the target nuclei.

It is interesting to observe that although it has already been shown [60, 61] that the nuclear and Coulomb breakups of ^{6}Li with the target mass and charge, respectively, increase with the target mass and charge, respectively, the effect of the breakup on the complete fusion is roughly target independent. The reason seems to be related with the predominance of delayed breakups over prompt breakup, where the former is the sequential breakup which occurs in two steps. The first step is the excitation of the projectile to a long-lived resonance above the breakup threshold. Then, the resonance decays into the breakup channel, when the projectile is already in an outgoing trajectory leaving the target region. Only prompt breakup, which occurs in a time scale of 10^{-22} s, may affect fusion, since the resonance life-time is much longer than the collision time. Actually, Santra et $al.$ [62] performed exclusive measurements for the breakup of ^{6}Li in collisions with ^{209}Bi and they found that the sequential breakup via the ^{6}Li 3^+ resonant state at 2.186 MeV, with $T_{1/2} = 2.7 \times 10^{-20}$ sec., predominates in the $\alpha + d$ fragmentation.

The lowest breakup threshold of the weakly bound projectile ^{7}Li is 2.467 MeV for the breakup channel of ^{7}Li $\rightarrow \alpha + t$. The CF functions for projectile ^{7}Li on different target nuclei as a function of x are shown in Fig. 2. The solid line represents the UFF. It can be seen from Fig. 2 that the CF functions are suppressed owing to the presence of the breakup process, which is similar to the results of ^{6}Li. The dotted line is the UFF multiplied by the $F_{\rm B.U.}$ of 0.67. The $F_{\rm B.U.}$ is a little smaller than the results from the literature which are shown in the fifth column of the Table I. Those results were obtained by comparing the CF cross sections with coupled channel calculations, except for the reaction for ^{7}Li on ^{165}Ho which was compared with the predictions of a SBPM [5, 12]. From Fig. 2, one can find that all the CF functions coincide with the dotted line. So, the suppression factors for the projectile ^{7}Li induced reactions are also independent of the target charge.

A similar explanation used for ^{6}Li for this behavior can be made for ^{7}Li. Shrivastava et $al.$ [63] made exclusive measurements of ^{7}Li breakup, in collisions with ^{65}Cu. They found that the yield of coincident alpha-deuteron was much larger than that for coincidences between alpha and triton, and the analysis of angular distributions provided clear evidence that the alpha-deuteron events arise from a two-step process: direct one-neutron stripping, leaving the projectile in the 3^+ resonance of ^{6}Li, followed by its decay into an alpha particle plus a deuteron. They concluded that the cross section for the two-step
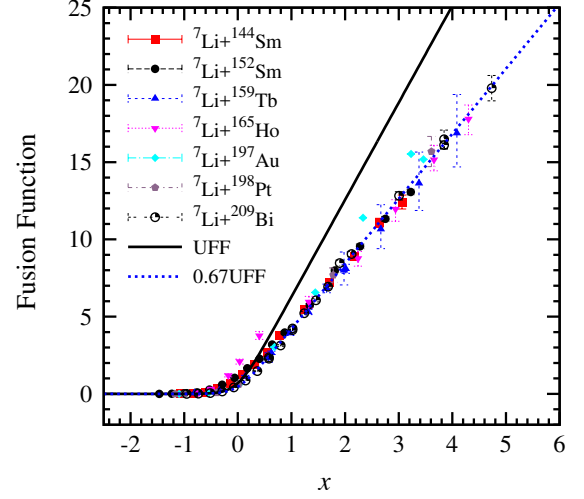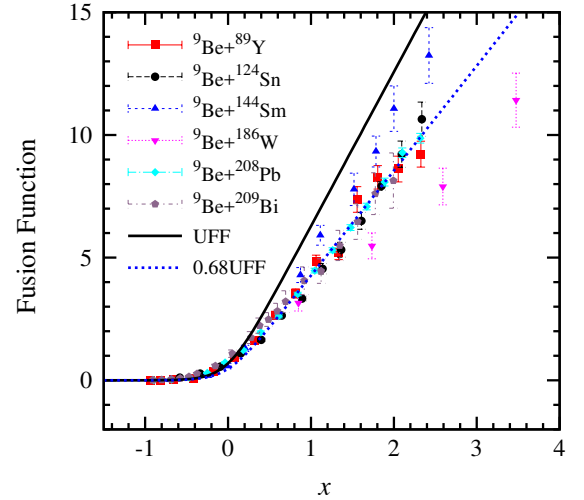

FIG. 2. (Color online) The complete fusion function $F(x)$ for the weakly bound projectile ^{7}Li on different target nuclei as a function of x. The solid line represents the UFF [Eq. (5)] and the dotted line is the UFF multiplied by the suppression factor $F_{\rm B.U.} = 0.67$ [cf. Eq. (7)]. The experimental values are taken from Refs. [25] (^{144,152}Sm), [4] (^{159}Tb), [5] (^{165}Ho), [24] (^{197}Au), [52] (^{198}Pt), and [10] (^{209}Bi).

FIG. 3. (Color online) The complete fusion function $F(x)$ for the weakly bound projectile ^{9}Be on different target nuclei as a function of x. The solid line represents the UFF [Eq. (5)] and dotted line is the UFF multiplied by the suppression factor $F_{\rm B.U.} = 0.68$ [cf. Eq. (7)]. The experimental values are taken from Refs. [28] (^{89}Y), [7, 53] (^{144}Sm), [54] (^{124}Sn), [9] (^{186}W), [10] (^{208}Pb), and [55, 56] (^{209}Bi).

breakup process was much larger than that for the direct breakup.

The CF functions for the weakly bound projectile ^{9}Be on targets ^{89}Y [28], ^{144}Sm [7, 53], ^{124}Sn [54], ^{186}W [9], ^{208}Pb [10], and ^{209}Bi [55, 56] are plotted in Fig. 3. The lowest breakup threshold of ^{9}Be is 1.573 MeV for its breakup into $n+\alpha+\alpha$. In Fig. 3, the solid line represents

the UFF, and the dotted line denotes the UFF scaled by the $F_{\text{B.U.}}$ of 0.68. The data of ^{9}Be on ^{144}Sm and ^{186}W are not included in the fitting. One can see that most of CF functions are very close to the dotted line, which is consistent with the results of ^{6,7}Li. The present suppression factor $F_{\text{B.U.}}$ is consistent with the factors obtained by comparing the CF data with the coupled channel calculations [10, 28, 54] and a SMPB [56]. It seems that the suppression factor should be smaller for ^{9}Be on ^{144}Sm and larger for ^{9}Be on ^{186}W. The systematic behavior of CF suppression of the weakly bound projectile ^{9}Be incident ^{144}Sm, ^{168}Er, ^{186}W, ^{196}Pt, ^{208}Pb, and ^{209}Bi was also explored based on a three-body classical trajectory model with stochastic breakup in Ref. [64]. The authors suggested that the discrepancy between ^{144}Sm and other targets may be attributed to the fact that the measured ICF cross section was only a lower limit and concluded that the suppression factor is nearly independent of the target charge. In Ref. [17], the systematic behavior of CF suppression of the weakly bound projectile ^{9}Be incident ^{89}Y, ^{124}Sn, ^{144}Sm, and ^{208}Pb was also investigated by comparing with the UFF, it was concluded that the systematic behavior for the CF suppression as a function of the target charge is not clear, which may be explained by different effects of transfer channels, especially one-neutron stripping, on the CF or TF.

Again, for ^{9}Be, Hinde et $al.$ [65] performed coincidence experiments to determine time scales in the breakup of ^{9}Be, in collisions with a ^{208}Pb target at sub-barrier energies. They were able to disentangle prompt ^{9}Be breakup from the delayed breakup of ^{8}Be, triggered by a one-neutron stripping process. In the latter case, the transfer reaction produces the unstable ^{8}Be nucleus, which has the half-life $T_{1/2} = 10^{-16}$ s, several orders of magnitude longer than the collision time, and so a process of this kind cannot influence fusion.

Figure 4 shows the CF functions for the weakly bound projectile ^{10}B on ^{159}Tb and ^{209}Bi targets. The data for ^{10}B with ^{159}Tb and ^{209}Bi are taken from Refs. [57] and [13], respectively. The most favorable breakup channel for ^{10}B is ^{10}B $\rightarrow$ ^{6}Li $+ \alpha$, of which the breakup threshold is 4.461 MeV. The CF functions for ^{10}B on target ^{159}Tb coincide with those for target ^{209}Bi. The CF functions lie below the UFF, as expected, which can be assigned to the breakup effects on the fusion process. The suppression factor is obtained as 0.8 by making a fit. This $F_{\text{B.U.}}$ is a little smaller than that of 0.85 which is obtained by comparing the CF cross sections with the predictions of a SBPM [13]. One can find that $F_{\text{B.U.}}$ for ^{10}B is larger than those for ^{6,7}Li and ^{9}Be, because ^{10}B has a larger breakup threshold.

Next we further investigate the effects of breakup coupling on CF reactions with tightly bound nucleus as a projectile. The CF functions for projectile ^{11}B on ^{159}Tb and ^{209}Bi targets are shown in Fig. 5. The data are taken from Refs. [57] for ^{159}Tb and [13] for ^{209}Bi, respectively. For the nuclide ^{11}B, the breakup threshold energy is 8.665 MeV for the most favorable breakup channel of
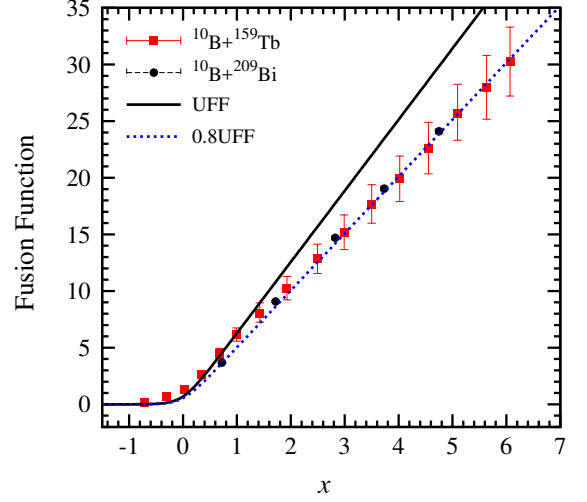

FIG. 4. (Color online) The complete fusion function $F(x)$ for the weakly bound projectile ^{10}B on different target nuclei as a function of x. The solid line represents the UFF [Eq. (5)] and the dotted line is the UFF multiplied by the suppression factor $F_{\text{B.U.}} = 0.8$ [cf. Eq. (7)]. The experimental data are from Refs. [57] (^{159}Tb) and [13] (^{209}Bi).
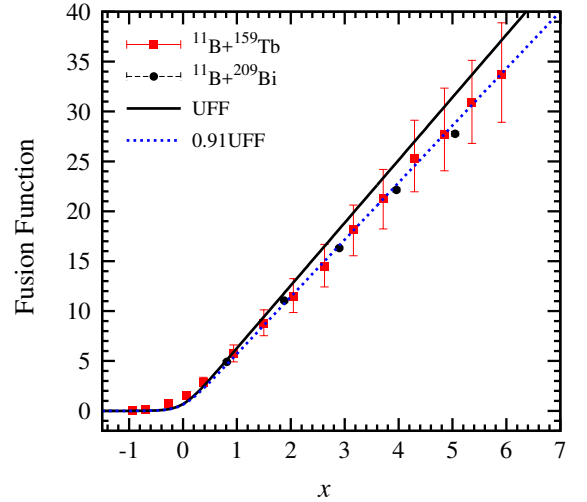

FIG. 5. (Color online) The complete fusion function $F(x)$ for the tightly bound projectile ^{11}B on different target nuclei as a function of x. The solid line represents the UFF [Eq. (5)] and the dotted line is the UFF multiplied by the suppression factor $F_{\text{B.U.}} = 0.91$ [cf. Eq. (7)]. The experimental values are from Refs. [57] (^{159}Tb) and [13] (^{209}Bi).

^{11}B $\rightarrow$ ^{7}Li $+ \alpha$. From the comparison between the CF functions and the UFF, it is found that the CF functions coincide with the UFF scaled by the $F_{\text{B.U.}}$ of 0.91 which is displayed by the dotted line. Comparing with the results for its neighboring nuclide ^{10}B, we find that the suppression factor is larger, as well as the breakup threshold, which is similar to the cases of ^{6,7}Li.

The CF functions of reactions with ^{12}C as a projectile are illustrated in Fig. 6. The lowest energy breakup
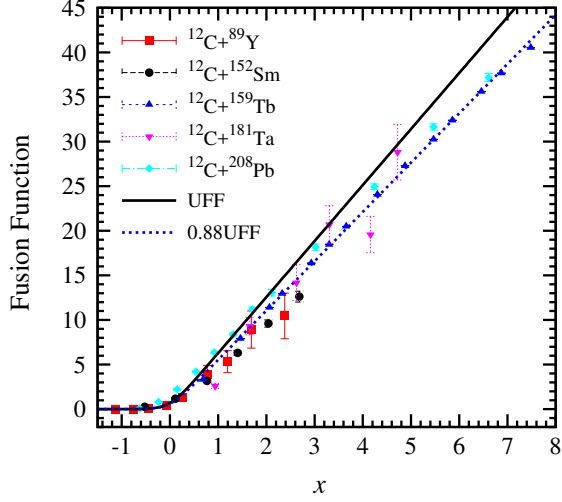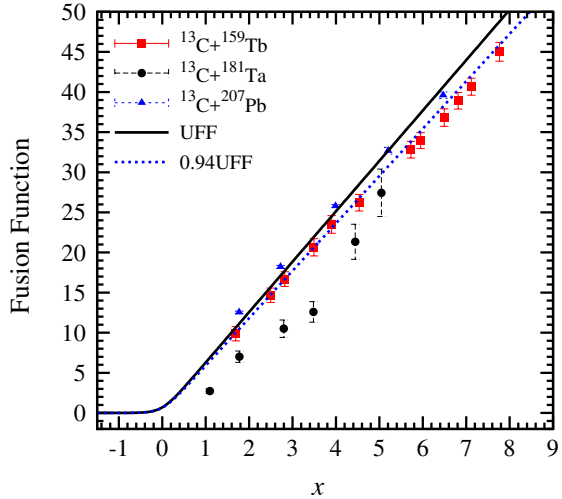
FIG. 6. (Color online) The complete fusion function $F(x)$ for tightly bound projectile ^{12}C on different target nuclei as a function of x. The solid line represents the UFF [Eq. (5)] and the dotted line is the UFF multiplied by the suppression factor $F_{\rm B.U.} = 0.88$ [cf. Eq. (7)]. The experimental values are taken from Refs. [28] (^{89}Y), [4] (^{152}Sm), [30] (^{159}Tb), [58] (^{181}Ta), and [14] (^{208}Pb).

FIG. 7. (Color online) The complete fusion function $F(x)$ for tightly bound projectile ^{13}C on different target nuclei as a function of x. The solid line represents the UFF [Eq. (5)] and the dotted line is the UFF multiplied by the suppression factor $F_{\rm B.U.} = 0.94$ [cf. Eq. (7)]. The experimental values are taken from Refs. [29] (^{159}Tb), [58] (^{181}Ta), and [14] (^{207}Pb).

channel is ^{12}C $\rightarrow$ ^{8}Be $+ \alpha$ with a threshold energy 7.367 MeV. It can be seen that the CF functions are close to the UFF multiplied by the $F_{\rm B.U.}$ of 0.88. It is identical to the factor obtained for ^{12}C on ^{208}Pb by comparing with the predictions of a SBPM [14]. The suppression factor is larger than that of ^{10}B and smaller than that of ^{11}B, which is related to that the breakup threshold energy of ^{12}C is larger than that of ^{10}B and smaller than that of
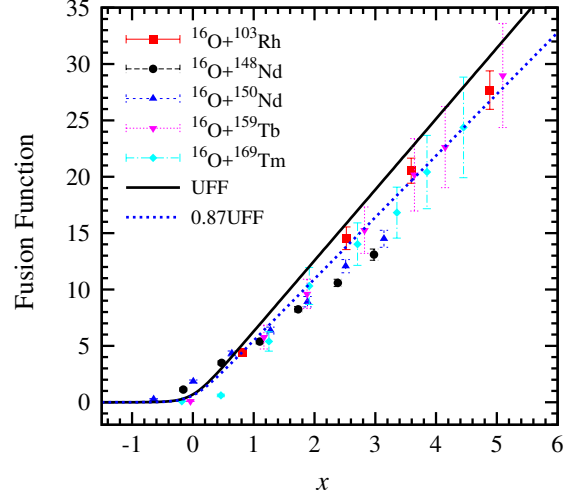

FIG. 8. (Color online) The complete fusion function $F(x)$ for tightly bound projectile ^{16}O on different target nuclei as a function of x. The solid line represents the UFF [Eq. (5)] and the dotted line is the UFF multiplied by the suppression factor $F_{\rm B.U.} = 0.87$ [cf. Eq. (7)]. The experimental values are taken from Refs. [59] (^{103}Rh), [4] (^{148,150}Nd), and [27] (^{159}Tb, ^{169}Tm).

^{11}B.

The CF data for the tightly bound projectile ^{13}C are also studied and the CF functions are shown in Fig. 7. For ^{13}C, the most favorable breakup channel is ^{13}C $\rightarrow$ ^{9}Be$+\alpha$, with a threshold energy of 10.648 MeV. The $F(x)$ for ^{13}C with ^{181}Ta is far below the UFF and not used in the fitting for the suppression factor. As expected, the suppression factor 0.94 is larger than that of ^{12}C and ^{11}B because of its larger threshold energy than those of ^{12}C and ^{11}B.

Figure 8 shows the CF functions for reactions with the tightly bound projectile ^{16}O. The threshold energy of ^{16}O is 7.162 MeV for the lowest energy breakup channel, ^{16}O $\rightarrow$ ^{12}C $+ \alpha$. The suppression factor is smaller than that of ^{12}C because of a lower breakup threshold compared to ^{12}C. From Fig. 8, it can be seen that the CF functions of ^{16}O on ^{103}Rh, ^{159}Tb, and ^{169}Tm are very close to the dotted line which is the UFF multiplied by the $F_{\rm B.U.}$ of 0.87. The suppression effect is also independent of the target charge, which is consistent with the results of ^{6,7}Li, ^{10,11}B, ^{9}Be, and ^{12}C. The results of CF functions of ^{16}O $+$ ^{148,150}Nd, which are not included in the fitting, lie far below the dotted line. Actually the TF functions also lie below the UFF. We expect new experimental investigations of these reactions.

B. Systematics of suppression factors

Based on the above analysis and discussions, one can conclude that the CF suppression for the reactions induced by the same nuclide is independent of the target
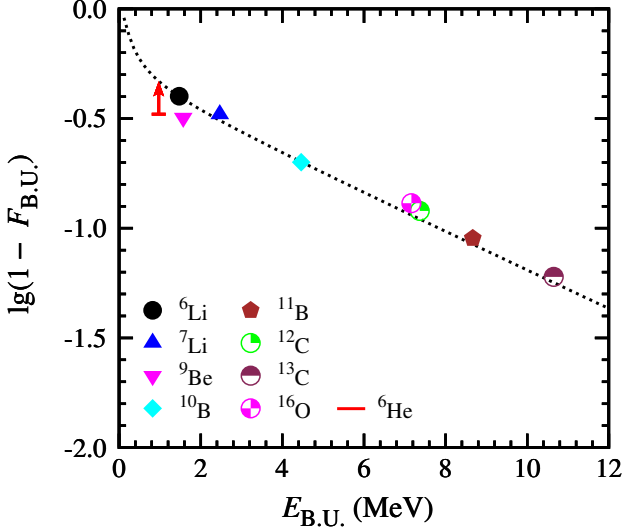
FIG. 9. (Color online) The suppression factors for projectiles ^{6,7}Li, ^{9}Be, ^{10,11}B, ^{12,13}C, and ^{16}O as a function of the lowest projectile breakup threshold ($E_{\text{B.U.}}$) for reactions on different targets. The solid line represents the suppression factor of total fusion for reactions with ^{6}He as a projectile. The dotted line denotes empirical formula (9).

charge. The suppression factors and the breakup threshold energies for ^{6,7}Li, ^{9}Be, ^{10,11}B, ^{12,13}C, and ^{16}O projectiles are listed in Table I. One can find that the suppression factor is sensitive to the breakup threshold energy of the projectile. Therefore, it is necessary to explore the relation between the suppression factor and the breakup threshold. This has been done by investigating the reactions with lead and bismuth targets [13, 14]. We will study this question with more reaction systems.

The suppression factors for projectiles ^{6,7}Li, ^{9}Be, ^{10,11}B, ^{12,13}C, and ^{16}O are shown as a function of the lowest projectile breakup threshold in Fig. 9. One can see that ^{6}Li induced reactions have the strongest suppression ($F_{\text{B.U.}} = 0.6$), and ^{13}C has the largest suppression factor of 0.94. This is because of ^{6}Li having the lowest breakup threshold of 1.474 MeV and ^{13}C having the highest breakup threshold of 10.648 MeV. Figure 9 shows that there exists an exponential relation between the suppression factor and the breakup threshold energy, at least for 1.474 MeV $< E_{\text{B.U.}} <$ 10.648 MeV. Furthermore, if the breakup threshold energy becomes even larger, breakup effects would play an even smaller role and $F_{\text{B.U.}}$ should be close to 1. On the contrary, when the breakup threshold energy is negligible, the interaction (specially the long range Coulomb force) will break the projectile at very large distances. So no complete fusion will occur, i.e., $F_{\text{B.U.}} \approx 0$. An analytical formula that fulfills these physical limits is

$$\lg(1 - F_{\text{B.U.}}) = -a\exp(-b/E_{\text{B.U.}}) - cE_{\text{B.U.}}, \quad (8)$$

where a, b, and c are parameters to be determined. By fitting the suppression factors given in Table I and shown

in Fig. 9, we get the values for the three parameters, $a = 0.33$, $b = 0.29$ MeV and $c = 0.087$ MeV^{-1}. That is, this analytical formula reads

$$\lg(1 - F_{\text{B.U.}}) = -0.33\exp(-0.29/E_{\text{B.U.}}) - 0.087E_{\text{B.U.}}, \quad (9)$$

or equivalently,

$$\ln(1 - F_{\text{B.U.}}) = -0.76\exp(-0.29/E_{\text{B.U.}}) - 0.2E_{\text{B.U.}}, \quad (10)$$

where $E_{\text{B.U.}}$ is in the unit of MeV. The suppression factors obtained by these empirical formulas are also listed in Table I and shown in Fig. 9 as a dotted line. From Fig. 9, one can find that the $F_{\text{B.U.}}$ for ^{9}Be is a little larger than that suggested from the empirical formula. This analytical relation suggests that the influence of the breakup channel on the complete fusion is a threshold effect. The physics behind it is still unclear. Further experimental and theoretical studies are expected.

These conclusions may look, at a first sight, contradictory with recent experimental evidences that the sequential breakup of the weakly bound nuclei ^{6,7}Li and ^{9}Be, following neutron and proton transfer [63, 64, 66, 67] predominates over the direct breakup, at least at sub-barrier energies. If this is so, one might not expect such clear dependence of the complete fusion with the direct breakup threshold energy as shown in Eqs. (8-10). However, as we have pointed out previously, this sequential breakup is of the delayed type and cannot affect fusion. Therefore, the effect of breakup on fusion may indeed depend on the breakup threshold energy.

Finally we focus on a typical neutron halo nucleus, ^{6}He. The lowest energy breakup channel of ^{6}He is $\alpha + 2n$ with a threshold energy 0.972 MeV. Experimentally, only total fusion cross sections have been measured [68, 69]. It is interesting to note that, with the UFF as a standard reference, the TF of reaction systems with ^{6}He as a projectile is also suppressed by the breakup and the TF suppression factor $F_{\text{B.U.}}^{\text{TF}}$ is 0.67 [70] (cf. Ref. [36] where this suppression factor was 0.7). This TF suppression factor is also shown in Fig. 9. One can find that $\lg(1 - F_{\text{B.U.}}^{\text{TF}})$ of ^{6}He is below the prediction of the empirical formula (9). Since CF cross sections must be smaller than TF cross sections, the CF suppression factor for ^{6}He should be smaller than the TF suppression factor. That is, 0.67 can only be treated as an upper limit of the CF suppression factor for ^{6}He and $\lg(1 - F_{\text{B.U.}})$ should be closer to that from the empirical formula (9). More efforts should be devoted to measuring the CF cross sections reaction systems with ^{6}He as a projectile.

IV. SUMMARY

In order to investigate the influence of breakup on the complete fusion (CF) at energies above the Coulomb barrier, we adopt the double folding and parameter-free São Paulo potential to get the barrier parameters of the reactions induced by the weakly or tightly bound projectiles.

The barrier parameters are used to extract the dimensionless fusion functions $F(x)$ from the CF cross sections for ^{6,7}Li, ^{9}Be, ^{10,11}B, ^{12,13}C, and ^{16}O induced reactions. Then the fusion functions $F(x)$ are compared with the universal fusion function (UFF). From the fact that the fusion function $F(x)$ is always below the UFF, we conclude that the CF cross sections are suppressed owning to the prompt breakup of projectiles. The CF suppression for the reactions induced by the same projectile is independent of target charge. The suppression factors for different projectiles are mainly determined by the lowest breakup thresholds. Based on the systematics obtained in this work, we propose an analytical formula which describes well the relation between the CF suppression factor and the breakup threshold energy.

[1] L. F. Canto, P. R. S. Gomes, R. Donangelo, and M. S. Hussein, Phys. Rep. **424**, 1 (2006).

[2] N. Keeley, R. Raabe, N. Alamanos, and J. Sida, Prog. Part. Nucl. Phys. **59**, 579 (2007).

[3] B. B. Back, H. Esbensen, C. L. Jiang, and K. E. Rehm, Rev. Mod. Phys. **86**, 317 (2014).

[4] R. Broda, M. Ishihara, B. Herskind, H. Oeschler, S. Ogaza, and H. Ryde, Nucl. Phys. A **248**, 356 (1975).

[5] V. Tripathi, A. Navin, K. Mahata, K. Ramachandran, A. Chatterjee, and S. Kailas, Phys. Rev. Lett. **88**, 172701 (2002).

[6] Z. H. Liu, C. Signorini, M. Mazzocco, M. Ruan, H. Q. Zhang, T. Glodariu, Y. W. Wu, F. Soramel, C. J. Lin, and F. Yang, Euro. Phys. J. A **26**, 73 (2005).

[7] P. R. S. Gomes, J. Lubian, B. Paes, V. N. Garcia, D. S. Monteiro, I. Padron, J. M. Figueira, A. Arazi, O. A. Capurro, L. Fimiani, A. E. Negri, G. V. Marti, J. O. Fernandez Niello, A. Gomez-Camacho, and L. F. Canto, Nucl. Phys. A **828**, 233 (2009).

[8] A. Shrivastava, A. Navin, A. Lemasson, K. Ramachandran, V. Nanal, M. Rejmund, K. Hagino, T. Ichikawa, S. Bhattacharyya, A. Chatterjee, S. Kailas, K. Mahata, V. V. Parkar, R. G. Pillay, and P. C. Rout, Phys. Rev. Lett. **103**, 232702 (2009).

[9] Y. D. Fang, P. R. S. Gomes, J. Lubian, X. H. Zhou, Y. H. Zhang, J. L. Han, M. L. Liu, Y. Zheng, S. Guo, J. G. Wang, Y. H. Qiang, Z. G. Wang, X. G. Wu, C. Y. He, Y. Zheng, C. B. Li, S. P. Hu, and S. H. Yao, Phys. Rev. C **87**, 024604 (2013).

[10] M. Dasgupta, P. R. S. Gomes, D. J. Hinde, S. B. Moraes, R. M. Anjos, A. C. Berriman, R. D. Butt, N. Carlin, J. Lubian, C. R. Morton, J. O. Newton, and A. Szanto de Toledo, Phys. Rev. C **70**, 024606 (2004).

[11] P. K. Rath, S. Santra, N. L. Singh, R. Tripathi, V. V. Parkar, B. K. Nayak, K. Mahata, R. Palit, S. Kumar, S. Mukherjee, S. Appannababu, and R. K. Choudhury, Phys. Rev. C **79**, 051601(R) (2009).

[12] V. Tripathi, A. Navin, V. Nanal, R. G. Pillay, K. Mahata, K. Ramachandran, A. Shrivastava, A. Chatterjee, and S. Kailas, Phys. Rev. C **72**, 017601 (2005).

[13] L. R. Gasques, D. J. Hinde, M. Dasgupta, A. Mukherjee, and R. G. Thomas, Phys. Rev. C **79**, 034605 (2009).

[14] K. Kalita, J. Phys. G: Nucl. Part. Phys. **38**, 095104 (2011).

[15] K. Hagino, A. Vitturi, C. H. Dasso, and S. M. Lenzi, Phys. Rev. C **61**, 037602 (2000).

[16] A. Diaz-Torres and I. J. Thompson, Phys. Rev. C **65**, 024606 (2002).

[17] P. R. S. Gomes, R. Linares, J. Lubian, C. C. Lopes, E. N. Cardozo, B. H. F. Pereira, and I. Padron, Phys. Rev. C **84**, 014615 (2011).

[18] P. R. S. Gomes, D. R. Otomar, T. Correa, L. F. Canto, J. Lubian, R. Linares, D. H. Luong, M. Dasgupta, D. J. Hinde, and M. S. Hussein, J. Phys. G: Nucl. Part. Phys. **39**, 115103 (2012).

[19] V. V. Sargsyan, G. G. Adamian, N. V. Antonenko, W. Scheid, and H. Q. Zhang, Phys. Rev. C **86**, 054610 (2012).

[20] M. Boselli and A. Diaz-Torres, J. Phys. G: Nucl. Part. Phys. **41**, 094001 (2014).

[21] H. Kumawat, V. Jha, V. V. Parkar, B. J. Roy, S. K. Pandit, R. Palit, P. K. Rath, C. S. Palshetkar, S. K. Sharma, S. Thakur, A. K. Mohanty, A. Chatterjee, and S. Kailas, Phys. Rev. C **86**, 024607 (2012).

[22] P. K. Rath, S. Santra, N. L. Singh, K. Mahata, R. Palit, B. K. Nayak, K. Ramachandran, V. V. Parkar, R. Tri-

pathi, S. K. Pandit, S. Appannababu, N. N. Deshmukh, R. K. Choudhury, and S. Kailas, Nucl. Phys. A **874**, 14 (2012).

[23] M. K. Pradhan, A. Mukherjee, P. Basu, A. Goswami, R. Kshetri, S. Roy, P. R. Chowdhury, M. S. Sarkar, R. Palit, V. V. Parkar, S. Santra, and M. Ray, Phys. Rev. C **83**, 064606 (2011).

[24] C. S. Palshetkar, S. Thakur, V. Nanal, A. Shrivastava, N. Dokania, V. Singh, V. V. Parkar, P. C. Rout, R. Palit, R. G. Pillay, S. Bhattacharyya, A. Chatterjee, S. Santra, K. Ramachandran, and N. L. Singh, Phys. Rev. C **89**, 024607 (2014).

[25] P. K. Rath, S. Santra, N. L. Singh, B. K. Nayak, K. Mahata, R. Palit, K. Ramachandran, S. K. Pandit, A. Parihari, A. Pal, S. Appannababu, S. K. Sharma, D. Patel, and S. Kailas, Phys. Rev. C **88**, 044617 (2013).

[26] M. Dasgupta, L. R. Gasques, D. H. Luong, R. du Rietz, R. Rafiei, D. J. Hinde, C. J. Lin, M. Evers, and A. Diaz-Torres, Nucl. Phys. A **834**, 147c (2010).

[27] P. P. Singh, B. P. Singh, M. K. Sharma, Unnati, D. P. Singh, R. Prasad, R. Kumar, and K. S. Golda, Phys. Rev. C **77**, 014607 (2008).

[28] C. S. Palshetkar, S. Santra, A. Chatterjee, K. Ramachandran, S. Thakur, S. K. Pandit, K. Mahata, A. Shrivastava, V. V. Parkar, and V. Nanal, Phys. Rev. C **82**, 044608 (2010).

[29] A. Yadav, V. R. Sharma, P. P. Singh, R. Kumar, D. P. Singh, Unnati, M. K. Sharma, B. P. Singh, and R. Prasad, Phys. Rev. C **86**, 014603 (2012).

[30] A. Yadav, V. R. Sharma, P. P. Singh, D. P. Singh, M. K. Sharma, U. Gupta, R. Kumar, B. P. Singh, R. Prasad, and R. K. Bhowmik, Phys. Rev. C **85**, 034614 (2012).

[31] P. R. S. Gomes, L. F. Canto, L. Lubian, P. Lotti, L. C. Chamon, E. Crema, and J. M. B. Shorto, Nucl. Phys. A **834**, 151c (2010).

[32] M. Beckerman, M. Salomaa, A. Sperduto, J. D. Molitoris, and A. DiRienzo, Phys. Rev. C **25**, 837 (1982).

[33] D. E. DiGregorio, M. diTada, D. Abriola, M. Elgue, A. Etchegoyen, M. C. Etchegoyen, J. O. Fernandez Niello, A. M. J. Ferrero, S. Gil, A. O. Macchiavelli, A. J. Pacheco, J. E. Testoni, P. R. S. Gomes, V. R. Vanin, R. L. Neto, E. Crema, and R. G. Stokstad, Phys. Rev. C **39**, 516 (1989).

[34] P. R. S. Gomes, J. Lubian, I. Padron, and R. M. Anjos, Phys. Rev. C **71**, 017601 (2005).

[35] L. F. Canto, P. R. S. Gomes, J. Lubian, L. C. Chamon, and E. Crema, J. Phys. G: Nucl. Part. Phys. **36**, 015109 (2009).

[36] L. F. Canto, P. R. S. Gomes, J. Lubian, L. C. Chamon, and E. Crema, Nucl. Phys. A **821**, 51 (2009).

[37] R. Wolski, Phys. Rev. C **88**, 041603(R) (2013).

[38] J. R. Leigh, M. Dasgupta, D. J. Hinde, J. C. Mein, C. R. Morton, R. C. Lemmon, J. P. Lestone, J. O. Newton, H. Timmers, J. X. Wei, and N. Rowley, Phys. Rev. C **52**, 3151 (1995).

[39] J. Zhang, C. Wang, and Z. Ren, Nucl. Phys. A **864**, 128 (2011).

[40] J. O. Newton, R. D. Butt, M. Dasgupta, D. J. Hinde, I. I. Gontchar, C. R. Morton, and K. Hagino, Phys. Rev. C **70**, 024605 (2004).

[41] J. O. Newton, R. D. Butt, M. Dasgupta, D. J. Hinde, I. I. Gontchar, C. R. Morton, and K. Hagino, Phys. Lett. B **586**, 219 (2004).

[42] M. A. Cândido Ribeiro, L. C. Chamon, D. Pereira, M. S. Hussein, and D. Galetti, Phys. Rev. Lett. **78**, 3270 (1997).

[43] L. C. Chamon, D. Pereira, M. S. Hussein, M. A. Candido Ribeiro, and D. Galetti, Phys. Rev. Lett. **79**, 5218 (1997).

[44] L. C. Chamon, B. V. Carlson, L. R. Gasques, D. Pereira, C. De Conti, M. A. G. Alvarez, M. S. Hussein, M. A. Cândido Ribeiro, E. S. Rossi, and C. P. Silva, Phys. Rev. C **66**, 014610 (2002).

[45] L. R. Gasques, L. C. Chamon, D. Pereira, M. A. G. Alvarez, E. S. Rossi, C. P. Silva, and B. V. Carlson, Phys. Rev. C **69**, 034603 (2004).

[46] E. Crema, L. C. Chamon, and P. R. S. Gomes, Phys. Rev. C **72**, 034610 (2005).

[47] P. R. S. Gomes, J. Lubian, and L. F. Canto, Phys. Rev. C **79**, 027606 (2009).

[48] J. M. B. Shorto, P. R. S. Gomes, J. Lubian, L. F. Canto, S. Mukherjee, and L. C. Chamon, Phys. Lett. B **678**, 77 (2009).

[49] J. Lei, J. S. Wang, S. Mukherjee, Q. Wang, and R. Wada, Phys. Rev. C **86**, 057603 (2012).

[50] X. P. Yang, G. L. Zhang, and H. Q. Zhang, Phys. Rev. C **87**, 014603 (2013).

[51] C. Y. Wong, Phys. Rev. Lett. **31**, 766 (1973).

[52] A. Shrivastava, A. Navin, A. Diaz-Torres, V. Nanal, K. Ramachandran, M. Rejmund, S. Bhattacharyya, A. Chatterjee, S. Kailas, A. Lemasson, R. Palit, V. V. Parkar, R. G. Pillay, P. C. Rout, and Y. Sawant, Phys. Lett. B **718**, 931 (2013).

[53] P. R. S. Gomes, I. Padron, E. Crema, O. A. Capurro, J. O. F. Niello, A. Arazi, G. V. Marti, J. Lubian, M. Trotta, A. J. Pacheco, J. E. Testoni, M. D. Rodriguez, M. E. Ortega, L. C. Chamon, R. M. Anjos, R. Veiga, M. Dasgupta, D. J. Hinde, and K. Hagino, Phys. Rev. C **73**, 064606 (2006).

[54] V. V. Parkar, R. Palit, S. K. Sharma, B. S. Naidu, S. Santra, P. K. Joshi, P. K. Rath, K. Mahata, K. Ramachandran, T. Trivedi, and A. Raghav, Phys. Rev. C **82**, 054601 (2010).

[55] C. Signorini, Z. H. Liu, A. Yoshida, T. Fukuda, Z. C. Li, K. E. G. Löbner, L. Müller, Y. H. Pu, K. Rudolph, F. Soramel, C. Zotti, and J. L. Sida, Euro. Phys. J. A **2**, 227 (1998).

[56] M. Dasgupta, D. J. Hinde, S. L. Sheehy, and B. Bouriquet, Phys. Rev. C **81**, 024608 (2010).

[57] A. Mukherjee, S. Roy, M. Pradhan, M. Saha Sarkar, P. Basu, B. Dasmahapatra, T. Bhattacharya, S. Bhattacharya, S. Basu, A. Chatterjee, V. Tripathi, and S. Kailas, Phys. Lett. B **636**, 91 (2006).

[58] K. S. Babu, R. Tripathi, K. Sudarshan, B. D. Shrivastava, A. Goswami, and B. S. Tomar, J. Phys. G: Nucl. Part. Phys. **29**, 1011 (2003).

[59] U. Gupta, P. P. Singh, D. P. Singh, M. K. Sharma, A. Yadav, R. Kumar, B. Singh, and R. Prasad, Nucl. Phys. A **811**, 77 (2008).

[60] D. R. Otomar, P. R. S. Gomes, J. Lubian, L. F. Canto, and M. Hussein, Phys. Rev. C **87**, 014615 (2013).

[61] M. S. Hussein, P. R. S. Gomes, J. Lubian, D. R. Otomar, and L. F. Canto, Phys. Rev. C **88**, 047601 (2013).

[62] S. Santra, V. V. Parkar, K. Ramachandran, U. K. Pal, A. Shrivastava, B. J. Roy, B. K. Nayak, A. Chatterjee, R. K. Choudhury, and S. Kailas, Phys. Lett. B **677**, 139 (2009).

[63] A. Shrivastava, A. Navin, N. Keeley, K. Mahata, K. Ramachandran, V. Nanal, V. V. Parkar, A. Chatterjee, and S. Kailas, Phys. Lett. B **633**, 463 (2006).

[64] R. Rafiei, R. d. Rietz, D. H. Luong, D. J. Hinde, M. Dasgupta, M. Evers, and A. Diaz-Torres, Phys. Rev. C **81**, 024601 (2010).

[65] D. J. Hinde, M. Dasgupta, B. R. Fulton, C. R. Morton, R. J. Wooliscroft, A. C. Berriman, and K. Hagino, Phys. Rev. Lett. **89**, 272701 (2002).

[66] D. H. Luong, M. Dasgupta, D. J. Hinde, R. d. Rietz, R. Rafiei, C. J. Lin, M. Evers, and A. Diaz-Torres, Phys. Lett. B **695**, 105 (2011).

[67] D. H. Luong, M. Dasgupta, D. J. Hinde, R. du Rietz, R. Rafiei, C. J. Lin, M. Evers, and A. Diaz-Torres, Phys. Rev. C **88**, 034609 (2013).

[68] J. J. Kolata, V. Guimarães, D. Peterson, P. Santi, R. White-Stevens, P. A. DeYoung, G. F. Peaslee, B. Hughey, B. Atalla, M. Kern, P. L. Jolivette, J. A. Zimmerman, M. Y. Lee, F. D. Becchetti, E. F. Aguilera, E. Martinez-Quiroz, and J. D. Hinnefeld, Phys. Rev. Lett. **81**, 4580 (1998).

[69] J. J. Kolata, V. Guimarães, D. Peterson, P. Santi, R. White-Stevens, J. von Schwarzenberg, J. D. Hinnefeld, E. F. Aguilera, E. Martinez-Quiroz, D. A. Roberts, F. D. Becchetti, M. Y. Lee, and R. A. Kryger, Phys. Rev. C **57**, R6 (1998).

[70] L. F. Canto, P. R. S. Gomes, R. Donangelo, J. Lubian, and M. S. Hussein, Phys. Rep., to be published (2014).